



ELSEVIER

Journal of Nuclear Materials xxx (2002) xxx–xxx

journal of
nuclear
materials

www.elsevier.com/locate/jnucmat

A new technique for the prediction of nonlinear material behavior

J.A. Wang, N.S. Rao

Oak Ridge National Laboratory, P.O. Box 2008, Building 6011, Oak Ridge, TN 37831-6370, USA

Received 17 April 2001; accepted 2 November 2001

7 Abstract

8 A new methodology is developed for the prediction of material behavior, such as aging processes, by utilizing a
9 combination of domain models and nonlinear estimators including neural networks and nearest neighbor regressions.
10 This methodology is applied to the problem of predicting embrittlement levels in light-water reactors by combining the
11 existing models with the conventional nonlinear estimators. The Power Reactor Embrittlement Database is used in this
12 study. The results indicate that the combined embrittlement predictor achieved about 56.5% and 32.8% reductions in
13 the uncertainties for General Electric Boiling Water Reactor plate and weld data compared to Regulatory Guide 1.99,
14 Revision 2, respectively. The implications of irradiation temperature effect to the development of radiation embrit-
15 tlement model are then discussed. © 2002 Published by Elsevier Science B.V.

16 *IDT:* E04; M02; P12; R03

17 *Keywords:* Radiation embrittlement; Reactor vessel integrity; Information fusion; Power reactor; Boiling water reactor; Material
18 modeling

19 1. Introduction

20 As we face the increasing electricity demand world-
21 wide and increasing concern about atmospheric emis-
22 sions, nuclear energy will be an important option within
23 a broad energy portfolio for industrialized and devel-
24 oping nations. The success of reactor technology de-
25 pends critically on the effective surveillance program to
26 monitor the degradation of irradiated materials during
27 service. The aging and degradation of light-water reac-
28 tor pressure vessels (RPVs) are of particular concern
29 because the magnitude of the radiation embrittlement is
30 extremely important to the plant's safety and operating
31 cost. Property changes in materials due to neutron-in-
32 duced displacement damage are a function of neutron
33 flux, neutron energy, and temperature, as well as the pre-
34 irradiation material history, material chemical compo-
35 sition and microstructure, since each of these influence
36 radiation-induced microstructural evolution. These fac-

tors must be considered to reliably predict RPV embrittlement and to ensure the structural integrity of the RPV. Based on the embrittlement predictions, decisions must be made concerning operating parameters, low-leakage-fuel management, possible life extension, and the potential role of pressure vessel annealing. Therefore, the development of embrittlement prediction models for nuclear power plants (NPPs) is a very important issue for the nuclear industry regarding the safety and lifetime extension of aging commercial NPPs.

Service failures due to inaccurate characterization of material aging responses could result in potentially costly repairs or premature component replacements, and in a worst-case could result in a catastrophic failure and loss of life. The general degradation mechanisms of the material aging behavior can be quite complicated and include: microstructure and compositional changes, time-dependent deformation and resultant damage accumulation, environmental attack and the accelerating

56 effects of elevated temperature, and synergistic effects of
57 all the above. These complex nonlinear dependencies
58 make the modeling of aging material behaviors a diffi-
59 cult task.

60 There have been several domain models that capture
61 various aspects for the material behavior; these models
62 are designed by the domain experts to capture various
63 critical relationships. At the same time, conventional
64 nonlinear estimators—while requiring very limited do-
65 main expertise—can model relationships that are not
66 readily apparent. Consequently, there has been a pro-
67 fusion of methods with complementary performance
68 with no single method proven to be always better than
69 all others. Our goal is to develop an effective method-
70 ology by combining the domain models with the non-
71 linear estimators including, neural networks and nearest
72 neighbor regressions (NNRs) to exploit their comple-
73 mentary strengths. We have previously developed a
74 large Power Reactor Embrittlement Database (PR-
75 EDB) [1] for US NPPs. Subsequently in cooperation
76 with the Electric Power Research Institute, additional
77 verification and quality assurance of the data were per-
78 formed by the US reactor vendors. PR-EDB is used in
79 this study to predict the embrittlement levels in light
80 water RPVs. The results indicate that our combined
81 predictor achieved about 56.5% and 32.8% reductions in
82 the embrittlement uncertainties for General Electric
83 (GE) Boiling Water Reactor (BWE) plate and weld data
84 compared to Regulatory Guide 1.99, Revision 2, re-
85 spectively.

86 More generally, this methodology offers a potential
87 for a new research field in material science for the de-
88 velopment of advanced materials through an under-
89 standing and/or modeling of the underlying mechanisms
90 of material aging. In particular, this approach holds a
91 promise for advances in material damage prediction of
92 structural components as, for example, in the develop-
93 ment of regulatory guidelines for managing surveillance
94 programs regarding the integrity of nuclear reactor
95 components.

96 In Section 2, we provide the background for the
97 proposed methodology. The objectives are presented in
98 Section 3. Various embrittlement models are briefly de-
99 scribed in Section 4. The fusion method is described in
100 Section 5, and the performance results are discussed in
101 Section 6.

102 2. Background

103 The complex nonlinear dependencies observed in
104 typical material embrittlement data, as well as the exis-
105 tence of large uncertainties and data scatter, make the
106 modeling of material behavior (such as embrittlement
107 prediction) a difficult task. The conventional statistical

108 and deterministic approaches have proven to result in
109 large uncertainties, in part because they do not fully
110 exploit the domain specific knowledge. The domain
111 models built by researchers in the field, on the other
112 hand, are not able to fully exploit the statistical and
113 information content of the data. As evidenced in previ-
114 ous studies, it is unlikely that a *single* method, whether it
115 is statistical, nonlinear or domain model will outperform
116 all others. Considering the complexity of the problem, it
117 is more likely that certain methods will perform best
118 under certain conditions. In this paper, we propose to
119 combine a number of methods such as domain models,
120 neural networks, and NNRs. The combined system has
121 the potential to perform at least as well as the best of the
122 constituents by exploiting the regions where the indi-
123 vidual methods are superior. Such combination methods
124 became possible due to recent developments in the
125 measurement-based optimal fusers [2–4] in the area of
126 information fusion.

127 The problem of estimating nonlinear relationships
128 from noisy data has been well studied in the area of
129 statistical estimation [5]. The nonlinear statistical esti-
130 mators such as the Nadaraya-Watson estimator and
131 regressograms [6] essentially rely on the properties of
132 regressions. While neural networks and statistical esti-
133 mators are general, the domain models developed by the
134 material scientists specifically capture the critical rela-
135 tionships in the data that are not easily amenable to
136 general methods. Such models are typically based on a
137 combination of linear and nonlinear models, which are
138 carefully chosen through an understanding of experi-
139 mental data.

140 Particularly among the models developed for em-
141 brittlement data, there is unlikely to be a single winner,
142 and different models perform well under different con-
143 ditions. By discarding one or more models, one stands
144 the risk of not characterizing certain critical perfor-
145 mance. We propose to combine various methods using
146 isolation fusers [5]. The most important part of these
147 fusers is that the combined system can be guaranteed to
148 be at least as good as the best individual estimator with a
149 specified probability. Furthermore, fusion of no proper
150 subset of the models performs better than the fused
151 system based on all models. This way the positive as-
152 pects of *all* individual estimators can be exploited
153 without discarding any single estimator.

154 We now briefly illustrate the overall fusion method to
155 highlight the underlying principle. Consider the follow-
156 ing target function, wherein the objective it to model this
157 function using the training data points obtained by
158 knowing the function values at certain values of x . The
159 prediction of each model is then tested using test data
160 points that are different from the training points. We
161 consider different estimators based on artificial neural
162 networks (ANN), where each estimator has a different

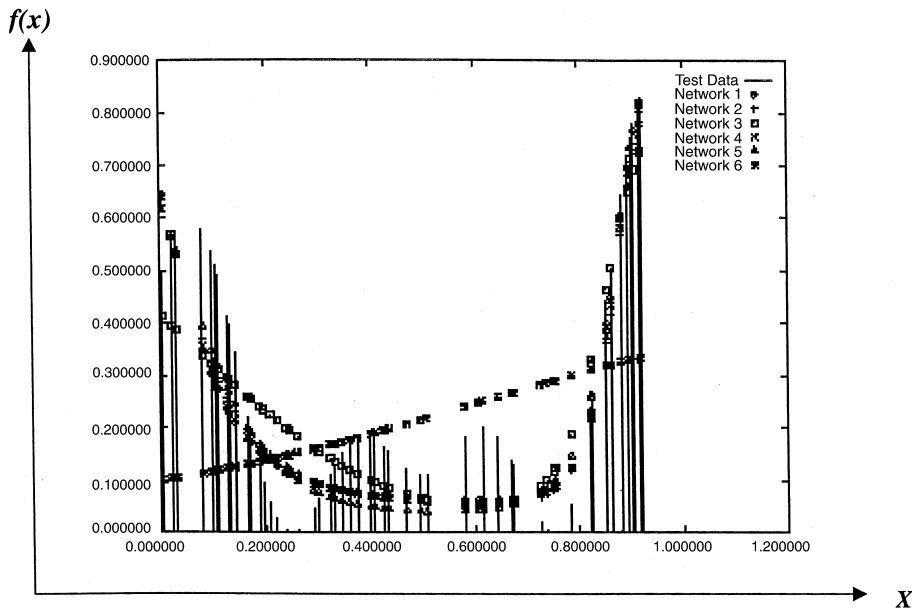


Fig. 1. Six ANN prediction models trained with backpropagation algorithm with different learning rates randomly chosen.

163 number of hidden nodes and different learning rate for
164 the backpropagation training algorithm.

$$f(x) = 0.02(12 + 3x - 3.5x^2 + 7.2x^3)(1 + \cos 4\pi x) \times (1 + 0.08 \sin 3\pi x) \quad (1)$$

166 Consider that we obtain six different neural network
167 estimators for the target function by randomly choosing
168 the number of hidden nodes and the learning rate pa-
169 rameters for the backpropagation algorithm. Each
170 neural network is trained with the same set of sample
171 points and tested on set of test points. The predictions of
172 the networks on the test data points are shown in Fig. 1.
173 The solid lines represent the actual function values, and
174 predictions by different neural networks are shown by
175 various other symbols. It is of interest to note that
176 network 4 appears to be a linear fit and the worst fit
177 among all networks. But, it is the only network that is
178 able to accurately model the function $f(x)$ at the
179 neighborhood of $x = 0.4$. We now combine the results
180 using linear and projective fusers, both of which are
181 special cases of the isolation fusers; their performance is
182 shown in Fig. 2. The linear fuser's output is shown in
183 dotted lines and the output of projective fuser is denoted
184 by +. Compared to the actual function values (test
185 data), both fusers perform similarly except around
186 $x = 0.4$. The projective fuser identified that one of the
187 neural network 4 performs better than other in this re-
188 gions and utilized to predict the function. Note that this
189 is the only region that this neural network performed
190 well, and projective fuser is able to exploit its superior
191 performance in this localized region. In terms of test

error, the linear fusers is 31.15 times better than best
ANN estimator and the projective fuser is 1.3 times
better than linear fuser. The summary of these results is
presented in Table 1, which shows that carefully chosen
fusers can achieve performance significantly better than
the individual estimators. In essence, both fusers are able
to achieve performance superior to the individual esti-
mators by 'exploiting' the performances of the individ-
ual estimators. In particular, both fusers are shown to
perform at least as good as the best of the estimators (in
terms of the test error).

For the embrittlement problem, the deployment of
these fusers on various models will ensure that the fused
model is at least as good as the best of the individual
models, irrespective of their individual performances.
However, the general results on fusers do not specify the
actual performance gains that may be achieved in a
particular application. We show here that significant
performance improvements are indeed obtained by em-
ploying fusers to combine various embrittlement mod-
els.

3. Objectives

Our objective is to combine various estimators for
predict the embrittlement behavior of irradiated materi-
als, and then combine them to exploit their comple-
mentary strengths. We employ neural networks, NNRs,
and domain models, based on the PR-EDB data, to
predict the transition temperature shift of RPV materi-

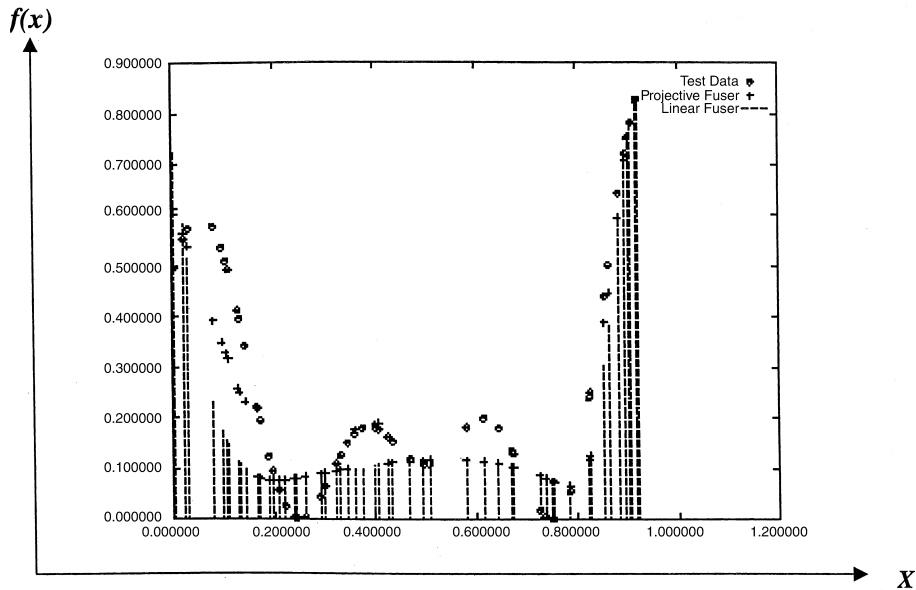


Fig. 2. Two information fusion models. In terms of test error, the linear fusers is 31.15 times better than the best ANN, and the projective fuser is 1.3 times better than the linear fuser.

Table 1
Summary of the simulation results for the information fusion technique

Data size		Projective as good ^a	Other better		Performance (times) ^b		Average error
Training	Test		Linear	Best	Linear	Best	
<i>Without noise</i>							
10	10	8	1	1	1.009269	10.489711	0.075042
25	25	8	2	0	1.039885	13.426878	0.021926
50	50	10	0	0	1.304039	31.157175	0.013454
75	75	10	0	0	1.530556	89.050201	0.004725
100	100	10	0	0	1.788104	87.905518	0.003764
<i>With noise</i>							
10	10	8	2	0	0.982823	9.205843	0.041874
25	25	8	2	0	1.045973	14.115362	0.026983
50	50	10	0	0	1.293410	19.121033	0.010399
75	75	9	1	0	1.275850	33.192585	0.008435
100	100	10	0	0	1.227069	37.937778	0.007115

^a For each dataset size, 10 different samples are utilized.

^b Projective fuser outperformed both linear fuser and the best estimators.

220 als, which is a measure of the material embrittlement.
 221 From the past experience [7], the boiling water has larger
 222 uncertainty compared to the other power reactor data.
 223 In this study, we only focused on the BWR data.
 224 The first task is to create unbiased training and test
 225 sets. The GE BWR surveillance data (listed in PR-EDB)
 226 were pre-processed and streamlined. The final processed
 227 GE BWR data were compared with that of the ASTM
 228 E10.02 subcommittee embrittlement database for consistency
 229 in the surveillance information, such as irradiation
 230 temperature, chemical composition, Charpy

231 impact test data fitting methodology, and power time
 232 history, etc. The processed GE BWR data has essentially
 233 the same neutron fluences, chemistry, and irradiation
 234 temperature data compared to that of ASTM E10.02
 235 database, with minor difference of transition temperature
 236 shift (within a few degree F). The GE BWRs data
 237 values were then scaled to the interval [-1,1] using a
 238 Linear Max/Min transformation. This ensures that no
 239 one component in the data dominates the parameter
 240 optimization scheme. Then the data were randomly
 241 partitioned into training and testing sets.

231
232
233
234
235
236
237
238
239
240
241

242 The second task consists of determining a number of
 243 estimators for this problem. For each method, a criteria
 244 function and optimization routine will be selected that
 245 consistently produces stable results. For statistical esti-
 246 mators, we will follow the procedure described in the
 247 literature. For ANN, one hidden layer and eleven hid-
 248 den nodes were chosen with 2000 epoch iteration. A
 249 random generator was used to generate the initial
 250 weights for ANN modeling. Four sets of ANN models
 251 were tested. We then combine the statistical and deter-
 252 ministic estimators using information fusion techniques.
 253 The combined system is guaranteed to perform at least
 254 as well as the best of the constituents by exploiting the
 255 regions where the individual methods are superior.

256 A novel methodology is developed here for inferring
 257 nonlinear relationships that are typical in material be-
 258 havior prediction. A tool based on this methodology is
 259 also implemented for the embrittlement prediction of
 260 NPPs. This tool could be expanded and adapted for use
 261 in other areas in which nonlinear material properties are
 262 important, such as failure analysis of highway bridges,
 263 airplane safety analyses, and others.

264 4. Embrittlement prediction models

265 In this section we briefly described various models
 266 used for embrittlement prediction, which will be com-
 267 bined in the next section.

268 4.1. ORNL embrittlement prediction models

269 The residual defects in materials due to neutron-in-
 270 duced displacement damage are a function of neutron
 271 energy, neutron flux, exposure temperature, and the
 272 material properties that determine how neutrons interact
 273 with atoms and how defects interact within the material
 274 [8]. Thus, temperature, neutron flux, neutron energy
 275 spectrum, and material composition and processing
 276 history all contribute to the radiation embrittlement
 277 process [9]. Insufficient considerations of these factors
 278 may result in misleading correlations and, thus, incor-
 279 rect predictions of material state and material behavior,
 280 as well as incorrect end-of-life determinations.

281 To minimize the influences of the uncertainty of the
 282 irradiation temperature, neutron energy spectrum, dis-
 283 placement rate, and plant operation procedures on em-
 284 brittlement models, improved embrittlement models
 285 based on group data that have similar radiation envi-
 286 ronments and reactor design and operation criteria are
 287 examined. The development of new embrittlement pre-
 288 diction equations [7,10] stem from a series of studies on
 289 radiation embrittlement models, such as Guthrie's
 290 model [11], Odette's model [12], Fisher's model [13],
 291 B&W Lowe's model [14], the French FIM model [15],

etc., and several other parameter studies on the PR-
 EDB. Although the copper-precipitation model has been
 extremely successful in explaining many aspects of ir-
 radiation embrittlement, it is becoming increasingly ev-
 ident that other elements also contribute to the
 embrittlement of the RPV steel, such as Ni, P, Mn, Mo,
 and S. Theoretically, all the impurities in low alloy steel
 are candidates to be included in the modeling. For ex-
 ample, C, Si, Mn, Mo, S, etc., were investigated in the
 test run, but including or excluding these elements did
 not affect the overall outcome of the statistical param-
 eters significantly; therefore, these parameters (or ele-
 ments) were not incorporated into final governing
 equations. Thus, Cu, Ni, and P were tentatively selected
 as key elements and were incorporated into the formula
 of the new prediction equations. Furthermore, the rea-
 son for separating weld and base metals is because the
 welds tend to show the enhanced degradation. And the
 welding process presents a possible region of physical
 and metallurgical discontinuity, and offers added chan-
 ces for the introduction of defects and undesirable
 components or stresses.

A nonlinear-least-squares fitting Fortran program
 was written for this study. The development of the pa-
 rameters for this new embrittlement model is based on
 statistical formulation chosen by computer iterations.
 To some extent, the physical mechanisms are embedded
 in the equations, such as the formulation of the fluence
 factor (FF). Two new prediction models for GE BWRs
 data were developed, where the fluence rate effect was
 considered in the second prediction model, and are de-
 scribed below:

Model 1

$$\begin{aligned} \Delta RTNDT \text{ (base)} &= [-94.8 + 411.9Cu + 247.3\sqrt{CuNi} \\ &\quad + 498P/Cu]f^{0.3216-0.001003 \ln f} \\ \Delta RTNDT \text{ (weld)} &= [420.9Cu + 134.6\sqrt{CuNi} \\ &\quad - 25.94P/Cu]f^{0.2478-0.01475 \ln f} \end{aligned} \quad (2)$$

Model 2

$$\begin{aligned} \Delta RTNDT \text{ (base)} &= \left[(13.62 + 318.1Cu - 58.75\sqrt{NiCu} \right. \\ &\quad \left. - 151.4P/Cu) f^{-0.4354-0.1285 \ln f} \right] \\ &\quad + \left[(18.44 - 49.13\sqrt{CuNi} - 17.22Cu \right. \\ &\quad \left. - 97.57P/Cu) f(-8.344 \right. \\ &\quad \left. - 0.7045 \ln f) \ln(t_i/600000) \right] \\ \Delta RTNDT \text{ (weld)} &= 1.075 \left[(1580Cu - 86.06\sqrt{NiCu} \right. \\ &\quad \left. + 43.55P/Cu) f^{0.6523+0.02866 \ln f} \right] \\ &\quad - 2.23 \left[(4.193Ni - 45.54Cu) f(-11.63 \right. \\ &\quad \left. - 0.4554 \ln f) \ln(t_i/600000) \right] \end{aligned} \quad (3)$$

292
293
294
295
296
297
298
299
300
301
302
303
304
305
306
307
308
309
310
311
312
313
314
315
316
317
318
319
320
321
322
323
324

326

328 where ΔT_{NDT} is the transition temperature shift in
329 °F; and neutron fluence f is in unit of 10^{19} n/cm² ($E > 1$
330 MeV), effective full power time, t_i , is in hour, and Cu,
331 Ni, P are in wt.%.

332 4.2. Regulatory Guide 1.99, Revision 2's model

333 The transition temperature shift of Reg. Guide 1.99,
334 Rev. 2's model [16] was also used in this study for
335 comparison purpose, which is described as below.

$$\Delta T_{NDT} = (CF)f^{(0.28-0.10\log f)} \quad (4)$$

337 where ΔT_{NDT} is the transition temperature shift in °F,
338 CF (°F) is the chemistry factor (given in the Table 1 and
339 Table 2 of Reg. Guide 1.99, Revision 2), which is a
340 function of copper and nickel content, and neutron
341 fluence f is in unit of 10^{19} n/cm² ($E > 1$ MeV).

342 The residuals, defined as "measured shift minus
343 predicted shift," for Reg. Guide 1.99, Rev. 2's model are
344 illustrated in Figs. 3 and 4 for base and weld, respec-
345 tively.

346 4.3. Eason's models

347 The developed embrittlement model by E.D. Eason
348 et al. (Eason's model) [17], was used in this study. The
349 Eason's trend curve of transition temperature shift was
350 developed based on the power reactor data, and is de-
351 scribed below.

$$\begin{aligned} \Delta T_{3op} &= ff_1(\phi t) + ff_2(\phi t)f(cc) \quad [^\circ\text{F}] \\ ff_1(\phi t) &= A \exp \left[\frac{1.906 \times 10^4}{T_c + 460} \right] (1 + 57.7P) \left[\frac{\phi t}{10^{19}} \right]^a \\ ff_2(\phi t) &= \frac{1}{2} + \frac{1}{2} \tanh \left[\frac{\log(\phi t + 5.48 \times 10^{12} t_i) - 18.29}{0.600} \right] \\ ff(cc) &= B(\text{Cu} - 0.72)^{0.682} (1 + 2.56\text{Ni}^{1.358}) \end{aligned} \quad (5)$$

Table 2
Two-sigma uncertainty of the embrittlement models for GE BWR data

Embrittlement model	Parameters					Two sigma of residual (°F)	
	Cu	Ni	ϕt	t_i	T_c	Base (64 points)	Weld (48 points)
Reg. Guide 1.99, Rev. 2	×	×	×			55.0	47.9
ORNL fuser Model I	×	×	×	×	×	23.9	32.2
ORNL fuser Model II	×	×	×	×		24.6	34.1
ORNL Model I	×	×	×			39.6	41.8
ORNL Model II	×	×	×	×		27.6	38.5
Eason's model	×	×	×	×	×	40.9	51.0
K-NNR model	×	×	×	×	×	39.1	41.4
ANN-4 model	×	×	×	×	×	56.4	78.8 ^a

^a | Residual | > 100 °F are not included in two-sigma uncertainty evaluation.

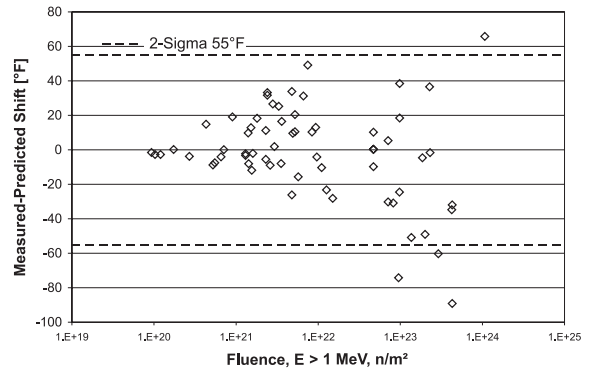


Fig. 3. Regulatory Guide 1.99, Revision 2's residual for GE BWR plate materials.

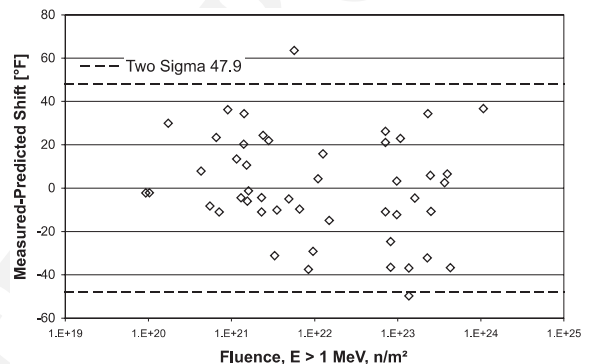


Fig. 4. Regulatory Guide 1.99, Revision 2's residual for GE BWR weld materials.

where

$$a = 0.4449 + 0.0597 \log \left[\frac{\phi t}{10^{19}} \right], \quad \phi t = \text{fluence}$$

353

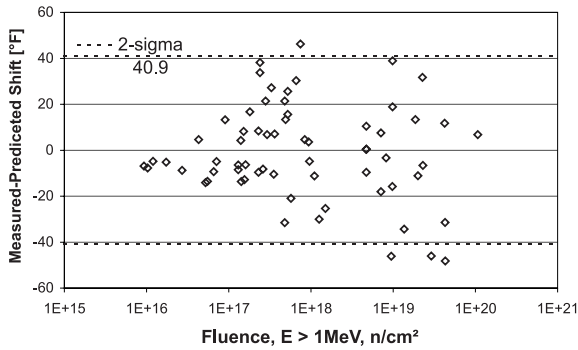


Fig. 5. Eason model's residual for GE BWR plate materials.

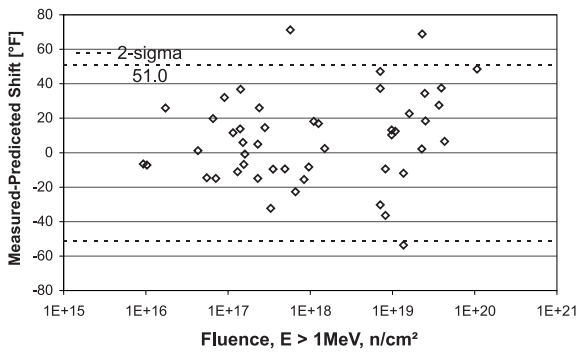


Fig. 6. Eason model's residual for GE BWR weld materials.

355 welds: $A = 1.10 \times 10^{-7}$, $B = 209$; plates: $A = 1.24 \times$
 356 10^{-7} , $B = 172$; forgings: $A = 0.90 \times 10^{-7}$, $B = 135$; T_c is
 357 coolant inlet temperature, °F.

358 The residual of Eason's model are illustrated in Figs.
 359 5 and 6 for base and weld, respectively.

360 4.4. ANN models

361 An ANN is a parameterized nonlinear mapping from
 362 an input space to an output space [18]. An ANN realizes
 363 mapping from an m -dimensional input space to an n -
 364 dimensional output space, and will have m nodes in its
 365 input layer and n nodes in its output layer. A multi-layer
 366 ANN (ML-ANN) is the most common architecture.
 367 This architecture has additional layers of nodes between
 368 the input and output layers. The information from each
 369 input-layer node is fanned out to nodes in the layer
 370 hidden between the input and output layers. The infor-
 371 mation entering a node in any hidden or output layer is
 372 the weighted sum of all information leaving the layer
 373 below it in the hierarchy. The node performs a trans-
 374 formation on the weighted information it receives and
 375 fans out the result to all nodes in the layer above it in the
 376 hierarchy (except for the output layer). The weighting

factors (weights) are free parameters that must be ad-
 377 justed to some chosen criteria function using some opti-
 378 mization algorithm. In this way, ANNs are able to
 379 capture many higher-order correlations that may exist in
 380 the data. The relationship between the higher-order
 381 correlations produces a nonlinear mapping. This is the
 382 reason ANNs may offer a more accurate prediction of
 383 material behaviors, embrittlement in this case. With
 384 methods like ANNs, one has a better tool to extract
 385 nonlinear relationships from embrittlement data to aid
 386 in the development of reliable maintenance and safety
 387 strategies and regulations in the nuclear industry.

The backpropagation algorithm is used to train the
 389 network with the data [18]. The training process deter-
 390 mines the weights of ANN to fit a suitable nonlinear map.
 391 The backpropagation's flexibility of ANN is why it
 392 does a better job of modeling than linear regression, but
 393 this method has several weaknesses. The backpropaga-
 394 tion algorithm is based on local descent and can get
 395 stuck in local minima, and as a result the predictive
 396 properties can be quite varied. Also, there are a number
 397 of tunable parameters such as starting weights and
 398 learning rates that have a significant effect on the weight
 399 computed by the back propagation algorithm. Thus,
 400 when different ANN models are trained with the same
 401 back propagation algorithm but with different starting
 402 weights and learning rates, the performance can be sig-
 403 nificantly different, as shown in Figs. 1 and 2. These
 404 networks however can be fused to achieve the perfor-
 405 mance of the best ANN [3].

Six independent variables, namely, Cu, Ni, P, fluence,
 407 irradiation temperature, and effective full power time
 408 were used in the ANN models. A program written in C
 409 language was used in this study.

410 4.5. K-nearest neighbor regression method

The NNR [5] is also chosen to generate an embrit-
 412 tlement model. The algorithm is described below. Let $x_1,$
 413 x_2, x_3, \dots, x_n be a sequence of n independent measure-
 414 ments with known classifications, and x be the mea-
 415 surement to be classified. Among $x_1, x_2, x_3, \dots, x_n,$ let the
 416 measurement with the smallest distance from x be de-
 417 noted as x' . Then the nearest-neighbor decision rule as-
 418 signs the classification of x' to that of x . As for K-nearest
 419 neighbor regression (K-NNR), it assigns to an unclas-
 420 sified sample point the class most heavily represented
 421 among its K nearest neighbors to x . In this study we
 422 chose the first three nearest neighbors with properly
 423 weighted function to represent the unclassified sample.

Six independent variables, namely, Cu, Ni, P, fluence,
 425 irradiation temperature, and effective full power time
 426 were used in K-NNR models. A second test K-NNR
 427 model, excluding irradiation temperature from the fit-
 428 ting parameter, generated a nearly identical trend curve
 429

430 as that with irradiation temperature. A program written
431 in C language was used in this study.

432 **5. Fusion of embrittlement models**

433 The development of this model consists of identifying
434 the error profiles of various estimators and the physical
435 parameters of the underlying problem, and designing the
436 fusers for combining the individual estimators. Here we
437 combined the statistical and deterministic estimators
438 using the linear fuser, which is a special case of the
439 isolation fusers [19]. The isolation fusers are shown to
440 perform probabilistically as good as best estimator
441 [4,19]. Given n estimators, $f_1(x), \dots, f_n(x)$, the linear
442 fuser is given by $f(x) = w_1 f_1(x) + \dots + w_n f_n(x)$, where
443 w_1, \dots, w_n are the weights. We computed the weights for
444 the fuser by minimizing the error of the fuser for the
445 training set. The program was written in C where the
446 solution is based on solving a quadratic programming
447 problem. In this study, we utilized the linear fuser to
448 develop the embrittlement models, six parameters,
449 namely, Cu, Ni, P, fast fluence, irradiation time, and
450 irradiation temperature, were incorporated into model
451 development.

452 **5.1. ORNL fuser model I**

453 Eight different models were investigated including
454 four neural network models, two ORNL models, one K-
455 NNR method, and the Eason's model. The results of the
456 ORNL linear fuser model indicate that this newly de-
457 veloped embrittlement model has about 56.5% and
458 32.8% reductions in uncertainties for GE BWR base and
459 weld data, respectively, compared to that of Reg. Guide
460 1.99, Rev. 2. These are significant improvements on the
461 embrittlement predictions for the RPV steels. The plots
462 of information model residual and its two-sigma un-

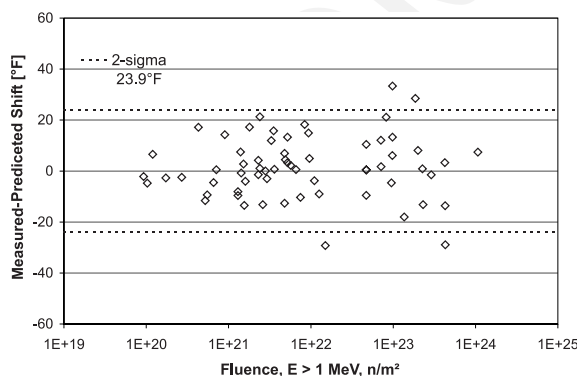


Fig. 7. ORNL-fuser model I overall residual for GE BWR base materials.

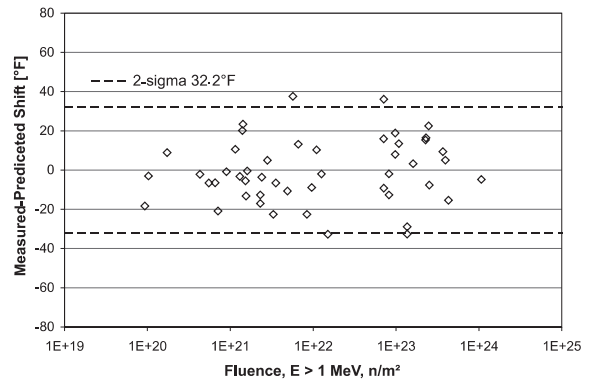


Fig. 8. ORNL-fuser model I overall residual for GE BWR weld materials.

certainties for base and weld materials are illustrated in 463
Figs. 7 and 8, respectively. 464

5.2. ORNL fuser model II 465

Fuser model II is a simplified version of fuser model 466
I, excluding the irradiation temperature from the fitting 467
parameter, and excluding the Eason's model from the 468
fusion modeling. The data scatter of residuals for fuser 469
model II are essentially the same as that of fuser model I. 470
The results of ORNL fuser model II indicate that it has 471
about 55.2% and 28.8% reduction in uncertainties for 472
GE BWR base and weld data, respectively, compared to 473
that of Reg. Guide 1.99, Rev. 2's model. This indicates 474
that fuser model I has marginal improved performance 475
compared to that of fuser model II. Thus, the impact of 476
irradiation temperature on embrittlement modeling for 477
GE BWRs surveillance data can be considered as sec- 478
ondary. 479

6. Discussion 480

The comparison of the performance of the embrittle- 481
ment models, based on the two-sigma uncertainty of 482
residual values, is stated in Table 2. the fuser model gave 483
the best performance among all the embrittlement pre- 484
diction models. ORNL embrittlement models indicates 485
that ORNL model II is superior to ORNL model I by 486
including irradiation time to simulate fluence-rate effect. 487
Thus, the implication of a flux effect in BWR environ- 488
ment was revealed in the model development. 489

Authors would like to point out that the fusion 490
modeling developed here is based on G.E. BWR data, 491
including 110 available sample data. Where, Reg. Guide 492
1.99/R2 and Eason's model were developed based on 493
both PWR and BWR surveillance data. Thus, the su- 494
perior prediction by ORNL fusion model comparing to 495

496 that of Reg. Guide 1.99/R2 and Eason's models may
497 also partially due to the subset of power reactor data
498 used in the model development. However, in the same
499 token, this study may also demonstrate the superiority
500 and advantage of using subset data, for example, the
501 vendor specific data, to develop power reactor embrittle-
502 ment model. (The reason is explained in the next pa-
503 ragraph.) In general a large data set with similar
504 characteristics or controllable parameters will generate a
505 better trend prediction compared to its subset. But a
506 misleading trend curve can result from a large data set
507 built upon different bases and uncontrollable parame-
508 ters, revealed by its large uncertainty.

509 The R.G. Guide 1.99/R2 was formulated based on
510 Guthrie's model and Odette's model and no temperature
511 effect was considered in embrittlement models develop-
512 ment, where, the FF and plates' chemistry factor (CF)
513 are from Guthrie's model [16]. 177 surveillance data
514 were used in Guthrie's model development, however,
515 only 6 data are from BWR environment. Thus, BWR
516 surveillance data may not be properly characterized
517 from Reg. Guide 1.99/2's model. From ASTM E10.02
518 database, the mean temperature and one standard de-
519 viation of BWR and PWR data are 540.3 ± 13.6 and
520 545.7 ± 10.4 °F, respectively. Therefore, from the irra-
521 diation temperature variability point, the sample tem-
522 perature environment of PWR and BWR are
523 comparable. Currently, there are four major commercial
524 power reactor vendors in the US, namely, Westing-
525 house, General Electric, Babcock & Wilcox, and Com-
526 bustion Engineering. Each vendor has its unique designs
527 and specific operating procedures. There are significant
528 problems associated with insufficient information, such
529 as the detailed irradiation temperature of surveillance
530 specimen and the thermal gradient within surveillance
531 capsules, and the lack of data in particular regions of
532 interests to characterize the vendor's service environ-
533 ments. About 64% of PR-EDB data is from Westing-
534 house; thus, the trend curve of all the four vendors' data
535 will closely resemble the Westinghouse plants' environ-
536 ment. Furthermore, B&W surveillance data appears to
537 experience higher irradiation temperature (based on
538 capsule melting wire) compared to other vendors, by
539 combining low and high temperature data may further
540 embedded bias on top of bias from the modeling point.
541 For example, from the trend curve of all the vendors'
542 data, the higher irradiation temperature data shows
543 negative bias (i.e. prediction model shows over-predic-
544 tion) and low irradiation data show positive bias.
545 However, the overall bias (or uncertainty) will cancel
546 each other resulting in a misleading statistical outcome,
547 such as its means and uncertainty.

548 Eason's model covers both PWR and BWR envi-
549 ronment, where 96 BWR data were included in model
550 development, and coolant inlet temperatures were in-

551 corporated into governing equations to simulate tem-
552 perature effect. In practice the coolant inlet temperature
553 is incorporated into the embrittlement model to simulate
554 the irradiation temperature for a pressurized light-water
555 reactor. However, a past study [9] showed that a large
556 bias can still be identified in Eason's model for surveil-
557 lance data from a higher irradiation temperature envi-
558 ronment, and the bias is similar to that of Regulatory
559 Guide 1.99, Rev. 2. [16]. This may indicate that the
560 coolant inlet temperature is not equivalent to the irra-
561 diation temperature experienced by the surveillance
562 specimens. Furthermore, from this study on fuser
563 models, neither including coolant inlet temperature or
564 excluding coolant inlet temperature has a significant
565 impact on the trend curve, which may further support
566 the above statement.

567 It is of interest to note that ORNL model I and K-
568 NNR model have very similar performance, however,
569 K-NNR model is generated more straightforward
570 without major efforts of refinement and reformulation of
571 the governing equation compared to that of ORNL
572 Model I.

573 For surveillance data, significant deviations of the
574 measured shift from the trend curve (i.e., more or less
575 than 34 °F for plate materials) should be considered as a
576 warning flag pointing to a possible anomalous capsule
577 environment. The large uncertainties are the result of
578 errors in the overall environment description. But, limit
579 attention has been given to characterizing the irradiation
580 temperature environment of the surveillance specimens.
581 In general, the neutron environment, fluence and flux,
582 can be determined fairly accurately, and possible effects
583 from these sources are relatively small in a power reactor
584 environment. However, the surveillance capsules' tem-
585 perature environments still heavily rely on the melting
586 wire's measurement. A more detailed analytical investi-
587 gation of specimen temperature is needed, based on
588 detailed neutronic and thermal-mechanical analysis for
589 specific capsule and specimen loading configuration, to
590 facilitate the RPV surveillance program in confidence.
591 Thus, in the current trend curve development, the most
592 likely reason for deviations from the trend curve is the
593 specimen temperature.

594 To develop a global embrittlement model for US
595 power reactors, an independent investigation of each
596 subgroup (each vendor) is recommended. Upon com-
597 pleting the investigations, if substantial improvement is
598 achieved for each subset based on the proposed meth-
599 odology, then information fusion technique will be uti-
600 lized to integrate all the subset models into a global RPV
601 embrittlement model.

602 7. Conclusions

603 We described an information fusion method for the
604 embrittlement prediction in light water RPVs, by combin-
605 ing domain models with, neural networks, and
606 nearest neighbor regressions. Our method resulted in
607 56.5% and 32.8% reduction in 2-sigma uncertainties
608 compared to that of the Reg. Guide 1.99, Rev. 2's
609 model, for base and weld materials, respectively. This
610 approach proved better than the ORNL embrittlement
611 models and other conventional models.

612 This new approach combines the conventional non-
613 linear methods and model based methods into an inte-
614 grated methodology applicable for modeling material
615 aging processes. This approach can potentially assist the
616 nuclear industry on the issues regarding safety and life-
617 time extension of aging commercial NPPs. By using a
618 wide spectrum of methods, the proposed tool can po-
619 tentially handle the subtle nonlinearities and imperfec-
620 tions, and can serve as a calibration and benchmark for
621 the existing models. The predictions generated by our
622 system have the potential for providing efficient, reliable,
623 and fast results, and can be an essential part of the
624 overall safety assessment of material aging research.

625 Future improvements of the proposed method can be
626 made through the development of the projective fusers
627 [3], which are based on a projective space that depends
628 on the underlying physical parameters. This class of
629 fusers is based on the lower envelope of the error re-
630 gression curves of various estimators such that the esti-
631 mator that forms the envelope is utilized in that region.

632 Acknowledgements

633 The authors gratefully acknowledge the efforts of R.
634 K. Nanstad for his valuable comments on this research.
635 This research is sponsored by the R&D Seed Money
636 Program of Oak Ridge National Laboratory, under
637 contract DE-AC05-00OR22725 with UT-Battelle, LLC.

638 References

- 639 [1] J.A. Wang, Embrittlement Data Base, Version 1, NUREG/
640 CR-6506 (ORNL/TM-13327), US Nuclear Regulatory
641 Commission, August 1997.
642 [2] N.S.V. Rao, J. Franklin Inst. 336 (2) (1999) 285.
643 [3] N.S.V. Rao, Multisensor fusion under unknown distribu-
644 tions: Finite sample performance guarantees, in: A.K.
645 Hyder (Ed.), Multisensor Fusion, Kluwer, Dordrecht,
646 2001.

- [4] N.S.V. Rao, IEEE Trans. Pattern Anal. Mach. Intell. 23 647
(8) (2001) 904. 648
- [5] R.O. Duda, P.E. Hart, D.G. Stork, Pattern Classification, 649
2nd ed., Wiley, New York, 2001. 650
- [6] N.S.V. Rao, V. Protopopescu, Proc. IEEE 84 (10) (1996) 651
1562. 652
- [7] J.A. Wang, in: Development of Embrittlement Prediction 653
Models for US Power Reactors, Effect of Radiation on 654
Materials: 18th International Symposium, ASTM STP 655
1325, American Society for Testing and Materials, Phila- 656
delphia, March 1999, p. 525. 657
- [8] L.K. Mansur, Mechanisms and kinetics of radiation effects 658
in metals and alloys, in: G.R. Freeman (Ed.), Kinetics of 659
Nohomogeneous Processes, 1987. 660
- [9] J.A. Wang, in: Analysis of the Irradiated Data for A302B 661
and A533B Correlation Monitor Materials, Effect of 662
Radiation on Materials: 19th International Symposi- 663
um, ASTM STP 1366, American Society for Testing 664
and Materials, Philadelphia, March 2000, p. 59. 665
- [10] J.A. Wang, F.B.K. Kam, F.W. Stallmann, in: Embrittle- 666
ment Data Base (EDB) and Its Applications, Effects of 667
Radiation on Materials: 17th Volume, ASTM STP 1270, 668
American Society for Testing and Materials, Philadelphia, 669
August 1996, p. 500. 670
- [11] G.L. Guthrie, Charpy Trend Curves Based on 177 PWR 671
Data Points, NUREG/CR-3391, US Nuclear Regulatory 672
Commission, 1983. 673
- [12] G.R. Odette, P.M. Lombrozo, J.F. Perrin, R.A. Wullaert, 674
Physically Based Regression Correlations of Embrittlement 675
Data From Reactor Pressure Vessel Surveillance Pro- 676
grams, EPRI NP-3319, Electric Power Research Institute, 677
1984. 678
- [13] S.B. Fisher, J.T. Buswell, A Model for PWR Pressure 679
Vessel Embrittlement, Berkeley Nuclear Laboratories, 680
Central Electric Generating Board, GL139PB, 1986. 681
- [14] A.L. Lowe Jr., J.W. Pegram, Correlations for Predicting 682
the Effects of Neutron Radiation on Linde 80 Submerged- 683
Arc Welds, BAW-1803, Rev. 1, May 1991. 684
- [15] C. Brillaud, F. Hedin, B. Houssin, A Comparison Between 685
French Surveillance Program Results and Predictions of 686
Irradiation Embrittlement, Influence of Radiation on 687
Material Properties, ASTM STP 956, 1987, p. 420. 688
- [16] P.N. Randall, Basis for Revision 2 of the US Nuclear 689
Regulatory Commissions Regulatory Guide 1.99, Radia- 690
tion Embrittlement of Nuclear Reactor Pressure Vessel 691
Steels: An International Review (Second Volume), ASTM 692
STP 909, 1986, p. 149. 693
- [17] E.D. Eason, J.E. Wright, G.R. Odette, Improved Embrit- 694
tlement Correlations for Reactor Pressure Vessel Steels, 695
NUREG/CR-6551, US Nuclear Regulatory Commission, 696
2000. 697
- [18] M.H. Hassoun, Fundamentals of Artificial Neural Net- 698
works, MIT Press, Cambridge, MA, 1995. 699
- [19] N.S.V. Rao, Finite sample performance guarantees of 700
fusers for function estimators, in: Information Fusion, vol. 701
1 (1), 2000, p. 35. 702